IAC-20-C1.4.13

LOW-THRUST MICROSPACECRAFT DELIVERY TO A LUNAR ORBIT AFTER THE LAUNCH TO GTO OR MEO

Mikhail Ovchinnikov[a], Maksim Shirobokov[b]*, Sergey Trofimov[c], Stas Barabash[d], Per-Erik Atterwall[e]

[a] *Space Systems Dynamics Department, Keldysh Institute of Science and Technology, 4 Miusskaya Pl., Moscow, Russia 125047*, ovchinni@keldysh.ru
[b] *Space Systems Dynamics Department, Keldysh Institute of Science and Technology, 4 Miusskaya Pl., Moscow, Russia 125047*, shmaxg@gmail.com
[c] *Space Systems Dynamics Department, Keldysh Institute of Science and Technology, 4 Miusskaya Pl., Moscow, Russia 125047*, trofimov@keldysh.ru
[d] *Swedish Institute of Space Physics, 1 Bengt Hultqvists Väg, Kiruna, Sweden SE-981 92*, stas.barabash@irf.se
[e] *Beyond Atlas Corporation, 7B Kevinge Strand, Danderyd, Sweden SE-182 57*, per-erik@attwik.se
* Corresponding Author

Abstract

In this research, we perform a feasibility study on how to deliver a microspacecraft to a lunar orbit by its own propulsion system. In order to avoid the unacceptably large fuel expenditure, a low-thrust engine with a high specific impulse is considered. Two launch options are commercially available on a regular basis: the launch from Kourou into a standard geostationary transfer orbit (GTO) and the launch from Baikonur or one of Chinese launch pads into an inclined medium Earth orbit (MEO). Both options are assessed from the viewpoint of radiation dose accumulated when repeatedly crossing the Van Allen belts. The mass penalty is calculated based on the required thickness of aluminum shielding provided by ESA's SPENVIS online interface. The MEO launch is proved to be much more efficient due to the high inclination which minimizes the total time spent in the most hostile near-equatorial zone. An extensive search for time-optimal and energy-optimal trajectories performed across different launch dates reveals the dependence of transfer performance characteristics (delta-v, time of flight) on the initial geometrical configuration of the Earth-Moon system. All the spiral trajectories end with capture into the specific lunar L1 halo orbit followed by a ballistic transfer to an unstable near-polar lunar orbit and its stabilization and lowering. The effect of including one or several resonant encounters with the Moon is analyzed. In the current study, two parameters are used to specify a spacecraft and its thruster: the initial thrust-to-weight ratio and the specific impulse. Several combinations of their values typical for micro- and nanospacecraft are considered, which covers the vast range of possible future missions.

Keywords: microspacecraft, low thrust, lunar transfer, optimal trajectory, resonant encounter, radiation protection

1. Introduction

Over the last decade, the number of small spacecraft projects for deep space exploration is steadily growing. The fundamental reason behind this tendency lies in the substantially increased endurance of available electronic commercial off-the-shelf components and actuators for micro- and nanosatellites. Along with the traditionally mentioned advantages of cheapness, production rapidity and simplicity, it opens the road for small spacecraft and their formations to a variety of sophisticated deep-space missions, both technology-testing and science. The main obstacle on this road is the delivery issue: even for the nearest destination, the Moon, a small spacecraft has to wait for a piggyback launch, which happens very rarely. Moreover, common inflexibility and unpredictability of piggyback launch parameters make the mission design very challenging. Propulsion is also a prerequisite. Most of the 13 CubeSats—the secondary payload of the first Space Launch System mission scheduled in 2021—must possess their own propulsion capability (thruster/sail) to reach the destination orbit after the lunar fly-by [1].

In this research, we consider another option of deep-space delivery—by continuous thrust starting from one of easily accessible near-Earth orbits. Two scenarios are investigated: the launch from the Guiana Space Center (Kourou, French Guiana) into a standard geostationary transfer orbit (GTO) and the launch from Baikonur or one of Chinese launch facilities into an inclined medium Earth orbit (MEO). First, the radiation analysis for both scenarios is conducted to estimate the required thickness of shielding for crossing the Van Allen belts. Then, the transfer trajectory optimization is performed for several case studies with different dynamical characteristics (the initial thrust-to-weight ratio and the specific impulse). A transfer scheme involving the intermediate L1 halo orbit is chosen. Such an intermediate orbit serves as a natural location for the spacecraft commissioning phase before the critical lunar orbit insertion operation. Furthermore, when properly selected, a lunar L1 halo orbit appears to be linked with near-polar orbits around the Moon. Upon stabilization and lowering, a near-polar science orbit of prescribed size can be achieved.

The paper is organized as follows. In Section 2, the problem statement is formulated, different scenarios and their parameters are outlined. Section 3 is devoted to the radiation analysis of two launch options. For the first leg of the transfer trajectory, when the spacecraft repeatedly crosses the radiation belts, the total ionizing dose (TID) is estimated using ESA's SPENVIS online interface. In Section 4, the details of the optimization process during the rest transfer phases are given. Section 5 contains the numerical results we obtained and their brief discussion. It is followed by conclusions in the final section.

2. Problem statement

To this day, the only small spacecraft that managed to leave a near-Earth orbit by its own propulsion system is SMART-1, the 367 kg minisatellite launched by ESA in 2003 [2]. The 73 mN plasma thruster provided about 0.2 mm/s^2 of thrust acceleration at the beginning of the mission [3]. For near-future microspacecraft missions, a similar or slightly lower level of thrust-to-weight ratio is of interest. Another important thruster characteristic, the specific impulse I_{sp} (the ratio of the effective exhaust velocity to the standard gravity), should be high enough to avoid the unacceptably large fuel expenditure and, at the same time, should not demand too much power. For a typical microspacecraft of 30-40 kg, the kinetic power carried away by the jet stream should not be greater than 50-80 W, so that the total power consumption by a low-thrust engine would not exceed 300-400 W. Considering these constraints, the following dynamical scenarios are chosen (the thrust acceleration a_t is given for the initial moment of time):

1) fast $\quad a_t = 0.18$ mm/s^2, $I_{sp} = 1700$ s

2) balanced $\quad a_t = 0.14$ mm/s^2, $I_{sp} = 3000$ s

3) slow $\quad a_t = 0.10$ mm/s^2, $I_{sp} = 4000$ s

The first scenario is close to what was in the SMART-1 mission, while the rest two scenarios aim at saving more fuel due to the higher specific impulse values.

Two launch options, further named GTO and MEO, are considered. The former corresponds to the injection into the widely used $i = 6$ deg elliptical GTO orbit (the Kourou launch). The latter assumes that the initial orbit is circular, with the inclination of 55 deg (see Table 1). Such a MEO can be reached for a launch from Baikonur or Xichang.

Table 1. Orbital elements of two initial orbits studied

	Perigee alt., km	Apogee alt., km	Inclin., deg	Argum. of perigee, deg
GTO	250	35,950	6	178
MEO	23,200	23,200	55	not defined

To explore the variations in the transfer performance for different launch conditions, we consider four months of 2024 (January, April, July, October) and within every month, four equidistant dates (1st, 8th, 15th, 22nd) have been picked. Such sampling allows us to catch the effect of lunisolar perturbations. Variations due to the different relative geometrical configuration of the Moon orbit and the initial spacecraft orbit for a given date are studied by varying the start time with a one-hour step.

In order to avoid the influence of the final lunar orbit choice on the transfer trajectory optimization results, we include the stage of ballistic capture into an intermediate halo orbit around the lunar L1 libration point. This orbit is selected so that the subsequent ballistic departure will lead to a near-polar lunar orbit. According to the results obtained previously [4], the $A_z = 35,000$ km halo orbit ensures an almost polar orbit with low perilune (Fig. 1). Therefore, the transfer ends with the departure along the unstable hyperbolic manifold of that halo orbit followed by stabilization and spiraling downward to the specified lunar orbit. The details of this last stage of lunar transfer are given in the next section.

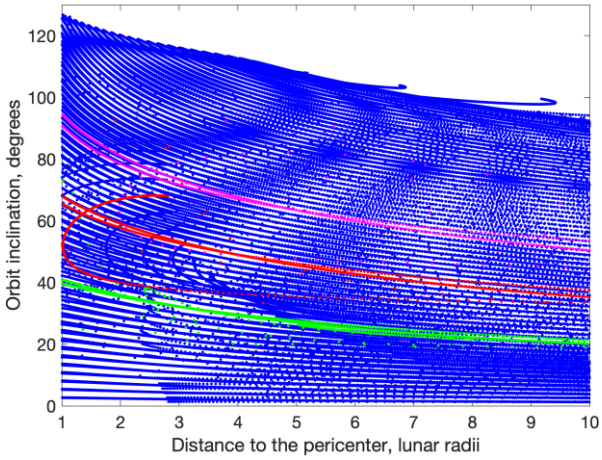

Fig. 1. Osculating inclination and perilune distance of lunar orbits after the departure from different points of various L1 halo orbits. Magenta dots correspond to the $A_z = 35,000$ km halo orbit, whereas red and green dots are respectively for the 25,000 km and 15,000 km halo orbits. The inclination is given with respect to the lunar orbit plane, so some variations are possible with respect to the selenographic (mean Earth-mean rotation) axes. The figure is taken from the authors' earlier paper [4].

After escaping from the dangerous zone of radiation belts, the spacecraft starts spiraling outward to get to the selected halo orbit. Two different optimization problems can be posed for this transfer stage: one can search for a time-optimal control which delivers the spacecraft to the stable manifold of the halo orbit; another option consists in minimizing the fuel expenditure. It is well known that

including one or several lunar encounters in the transfer scheme is capable of reducing the fuel cost. For the halo orbit considered, one of the most fuel-efficient chains of resonant encounters is 3:1 → 2:1 (see Fig. 2) [5, 6]. It is this chain whose efficiency we will test when designing a fuel-optimal transfer.

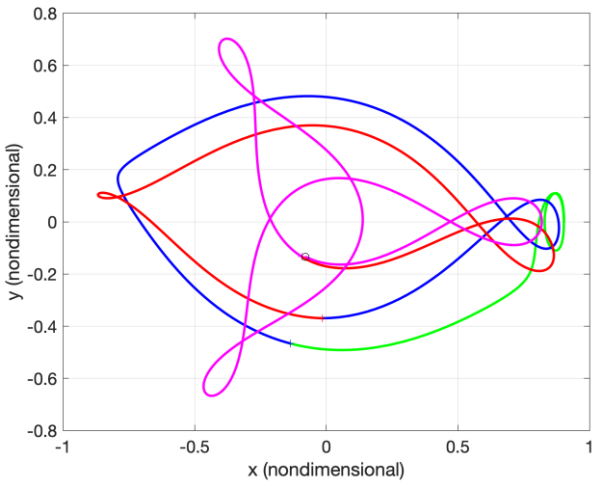

Fig. 2. The final part of the transfer trajectory including the resonant sequence 3:1 → 2:1 that ends with ballistic capture into the $A_z = 35,000$ km lunar L1 halo orbit [5]. The magenta color marks the 3:1 resonance trajectory. It is followed by the 2:1 resonance trajectory (colored red). After the final lunar encounter (located on the blue line), the spacecraft starts moving along the halo orbit's stable hyperbolic manifold (colored green) until it is captured.

3. Trajectory optimization process

From the above considerations and assumptions, any low-thrust transfer trajectory has the following structure. On the first leg, one aims at fastest pumping of the orbit altitude to escape the Van Allen belts. In all simulations, the near-optimal orbit raising by constantly applying the maximum thrust aligned with the inertial velocity vector is assumed (except for shadowed regions where the zero thrust is applied). The first leg is considered ended when the perigee altitude becomes greater than 40,000 km.

The second leg of the trajectory is a multi-revolution low-thrust transfer. The procedure of searching for time-optimal solutions is described in detail in [5]. Its essence consists in applying the maximum principle to the time-averaged variational equations of motion. The boundary condition at the end of the leg is formed by the values of orbital parameters for a stable manifold trajectory of the $A_z = 35,000$ km halo orbit propagated backward in time in the Earth direction until the perigee is reached.

If, instead of time optimization, we pose the problem of fuel optimization for a spiral trajectory on the second leg of the transfer, another optimization technique given in [6] is used. Assuming the thruster is ideally regulated (i.e., deep throttling is possible within the limited power range), the minimization of the fuel cost is equivalent to the minimization of the following functional:

$$\frac{1}{2}\int a_t^2 dt \to \min$$

The resulting solution is named energy-optimal. It gives the lower bound for the fuel cost in the case of a thruster with constant exhaust velocity. To solve for the energy-optimal control means to find a solution to the boundary value problem resulted from the maximum principle. In [6], the differential continuation method of solving such a problem is presented. It allows one to design a locally optimal transfer with a prescribed number of revolutions. The terminal condition for the second leg is set in such a way that the 3:1 → 2:1 sequence of resonant encounters (see Fig. 2) takes place followed by ballistic capture into $A_z = 35,000$ km halo orbit.

At the final stage of the lunar transfer, the spacecraft departs from the halo orbit toward the Moon. This stage can be calculated independently of the other parts of the transfer. Since the halo orbit was properly chosen, there exist unstable manifold trajectories leading to near-polar elliptical lunar orbits with a low perilune. To choose the best departure point in the halo orbit, we propagate 1000 unstable manifold trajectories. They start from different halo orbit points and significantly differ in their stability and geometrical properties. A simple retrothrust control was tried to be applied near the perilune (namely, within 10 lunar radii distance from the Moon's center of mass) to stabilize an orbit. Not every orbit can be stabilized by thrust of a given level; many trajectories collide with the Moon or leave the lunar vicinity. The problem of how to find the minimum thrust level needed to stabilize a low-energy unstable trajectory is far from trivial and requires additional study. Moreover, in the ephemeris model, the results turn out to be time-dependent—due to geocentric distance variations and lunar obliquity. Nonetheless, the general picture can be captured from the simulations for different dates. In the subplots of Fig. 3, a-b, the time of flight and fuel cost values are depicted for two different dates of departure from the halo orbit. The cost includes the fuel amount required for orbit stabilization followed by lowering until the perilune altitude drops to 1000 km. In average, 4 months and 3% of pre-departure total mass are to be reserved for this transfer stage. The inclination range covers various near-polar (83-97 deg) lunar orbits.

Since the last stage of the transfer is independent and does not influence the rest trajectory, in the next section, only the numerical results related to the first two legs of the transfer trajectory are discussed.

4. Results

Before proceeding to the description of optimization results obtained for the second leg of transfer trajectory, it is important to discuss the radiation protection issue.

4.1 Radiation analysis

For two initial orbits considered—GTO and MEO—and the balanced dynamical scenario ($a_t = 0.14$ mm/s^2, $I_{sp} = 3000$ s), we simulate the first trajectory leg where the tangential thrust is applied to get above the radiation belts. The trajectories obtained are then fed in the proper format to the SPace ENVironment Information System, SPENVIS, a special software developed and maintained by the Royal Belgian Institute for Space Aeronomy [7]. One of the main goals of SPENVIS is to be exploited by the European Space Agency for operational use in Earth and interplanetary missions.

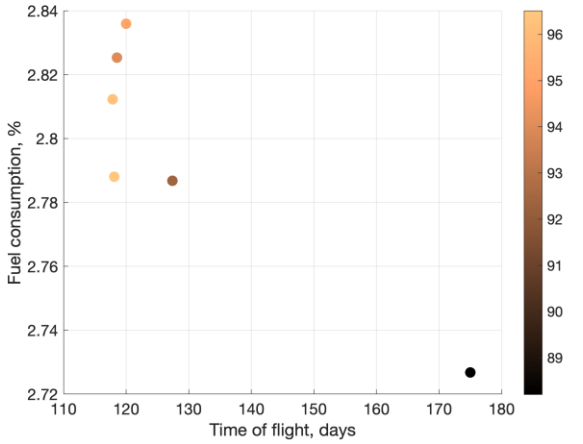

a)

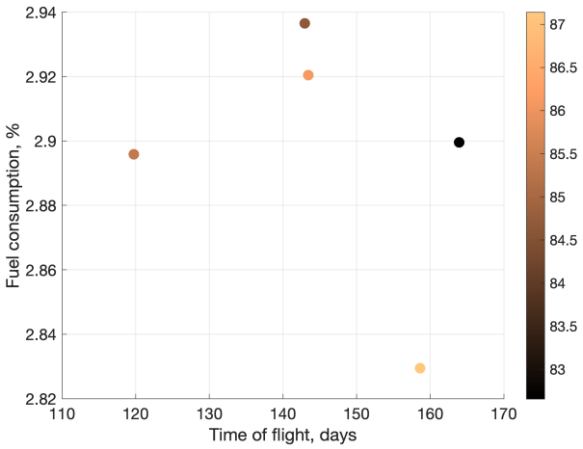

b)

Fig. 3. The performance of the last transfer leg (from the halo orbit departure to the arrival to a near-circular near-polar lunar orbit with a 1000 km perilune) for two dates of departure; balanced dynamical scenario assumed with $I_{sp} = 3000$ s. The color bar shows the inclination of the final lunar orbit w.r.t. the selenographic equatorial plane.

It was revealed that for all the GTO simulations, the required thickness of the aluminum shield is 4 mm (the maximum acceptable TID of 50 krad was adopted). It is equivalent to the mass penalty of about 1.1 g per square centimeter. The dimensions of a typical microspacecraft are assumed 25x25x50 cm, which leads to the total mass penalty of 6.1 kg.

When starting from MEO, the mass penalty is much lower: 2.5 mm aluminum shielding is enough to protect the microspacecraft (see the sample results in Figure 4). This gives 0.68 g of mass penalty per square centimeter, or 3.8 kg of the total penalty. Modern advanced plastics of low density (about 1 g/cm^3), especially with selective shielding, could reduce the mass penalty by 50%.

4.2 Comparing launch options and dynamical scenarios

To prove the superiority of the MEO launch over the GTO launch, it suffices to show that the performance of spiraling from the MEO is no worse than from the GTO. Indeed, the time-optimal transfer calculations reveal that the fuel consumption (proportional to the time of flight) is nearly the same for both options. Its partitioning over the first two transfer stages for the launch date of July 1 is presented in Fig. 5, a (GTO) and Fig. 5, b (MEO). An average fuel consumption of 10-11% of pre-launch total mass is observed for the balanced scenario, and the time of flight for the first two legs is 6-7 months.

To sum up, the higher mass penalty for the GTO due to the need of heavier shielding to protect from radiation remains largely uncompensated. In the rest of the paper, we discuss the MEO launch results only.

The comparison of the balanced dynamical scenario with the other two—fast and slow—demonstrates that it is the best compromise between the rapidity and the fuel cost. The fast scenario ($a_t = 0.18$ mm/s^2, $I_{sp} = 1700$ s) ensures a 1-2 months shorter flight, but demands almost twofold higher fuel consumption (Fig. 5, c). At the same time, the slow scenario, though saves additional 2-3% of the total mass for the payload (see Fig. 5, d), implies the much longer flight—up to 10 months.

4.3 Performance variations with launch date and time

Now let us move on to the influence of choosing the launch date and time on the transfer performance. When examining Figure 5, one can already notice performance variations depending on the choice of the start time. The most pronounced effect is for the highly inclined MEO. The start time defines the relative geometry of the lunar orbital plane and the plane of the initial spacecraft orbit. Their mutual orientation is especially critical in the case of significantly non-coplanar transfers, such as the ones we obtain for the 55 deg MEO.

Certain performance variations can also be attributed to the effect of the lunar gravity. It manifests itself in the slightly different cost when changing the launch date. In Fig. 6, the characteristics of the best trajectories for four dates throughout July 2024 are displayed. Variations up to 10% of the fuel mass are observed for the second leg.

Total mission dose (rad)

Al absorber thickness			Total	Trapped electrons	Brems-strahlung	Trapped protons	Tr. electrons+ Bremsstrahlung	Tr. el.+Bremss. +Tr. protons
(mm)	(mils)	(g cm^{-2})						
0.050	1.968	0.014	6.664E+06	6.652E+06	1.293E+04	-9.990E+02	6.665E+06	6.664E+06
0.100	3.937	0.027	3.916E+06	3.909E+06	8.430E+03	-9.990E+02	3.917E+06	3.916E+06
0.200	7.874	0.054	2.083E+06	2.078E+06	5.087E+03	0.000E+00	2.083E+06	2.083E+06
0.300	11.811	0.081	1.324E+06	1.321E+06	3.548E+03	0.000E+00	1.324E+06	1.324E+06
0.400	15.748	0.108	9.224E+05	9.197E+05	2.649E+03	0.000E+00	9.224E+05	9.224E+05
0.500	19.685	0.135	6.755E+05	6.734E+05	2.087E+03	0.000E+00	6.755E+05	6.755E+05
0.600	23.622	0.162	5.123E+05	5.106E+05	1.708E+03	0.000E+00	5.123E+05	5.123E+05
0.800	31.496	0.216	3.202E+05	3.190E+05	1.229E+03	0.000E+00	3.202E+05	3.202E+05
1.000	39.370	0.270	2.163E+05	2.153E+05	9.472E+02	0.000E+00	2.163E+05	2.163E+05
1.500	59.055	0.405	9.922E+04	9.864E+04	5.795E+02	0.000E+00	9.922E+04	9.922E+04
2.000	78.740	0.540	5.097E+04	5.056E+04	4.045E+02	0.000E+00	5.097E+04	5.097E+04
2.500	98.425	0.675	2.748E+04	2.717E+04	3.065E+02	0.000E+00	2.748E+04	2.748E+04
3.000	118.110	0.810	1.549E+04	1.524E+04	2.473E+02	0.000E+00	1.549E+04	1.549E+04
4.000	157.480	1.080	5.264E+03	5.082E+03	1.812E+02	0.000E+00	5.264E+03	5.264E+03
5.000	196.850	1.350	1.900E+03	1.755E+03	1.451E+02	0.000E+00	1.900E+03	1.900E+03
6.000	236.220	1.620	7.426E+02	6.196E+02	1.230E+02	0.000E+00	7.426E+02	7.426E+02

Fig. 4. Typical SPENVIS results for the first leg of the transfer trajectory starting from MEO

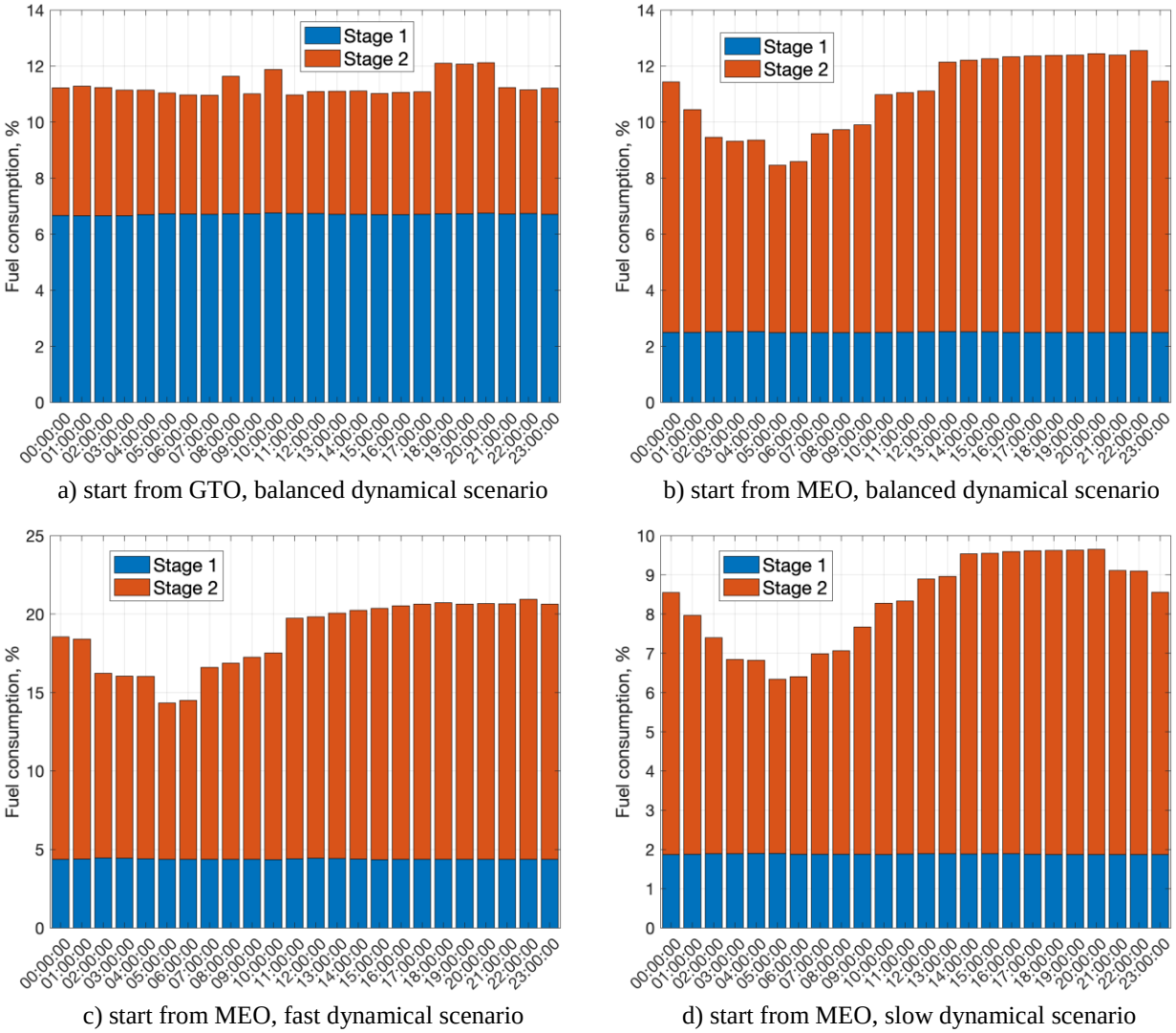

a) start from GTO, balanced dynamical scenario

b) start from MEO, balanced dynamical scenario

c) start from MEO, fast dynamical scenario

d) start from MEO, slow dynamical scenario

Fig. 5. Variation of the fuel consumption (relative to the pre-launch mass) for different start times on July 1, 2024

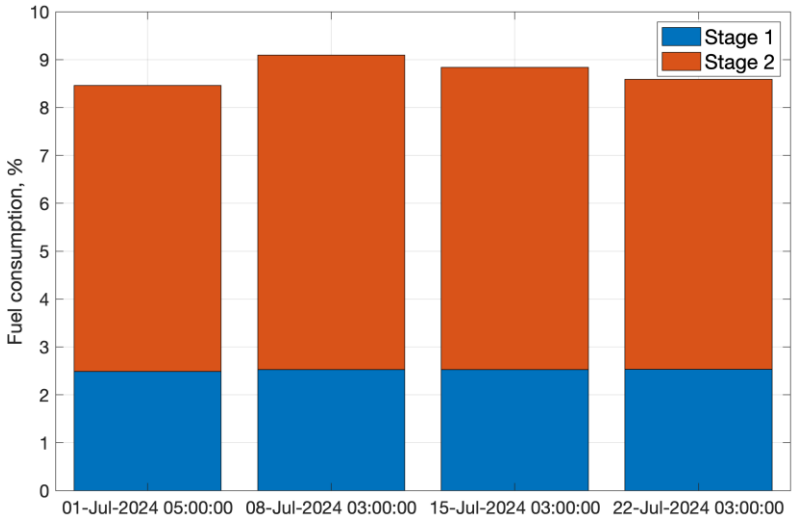

Fig. 6. Fuel consumption variation for different launch dates in July 2024 (MEO, balanced scenario). For each day, the fuel-optimal start time is selected and indicated below the corresponding bar.

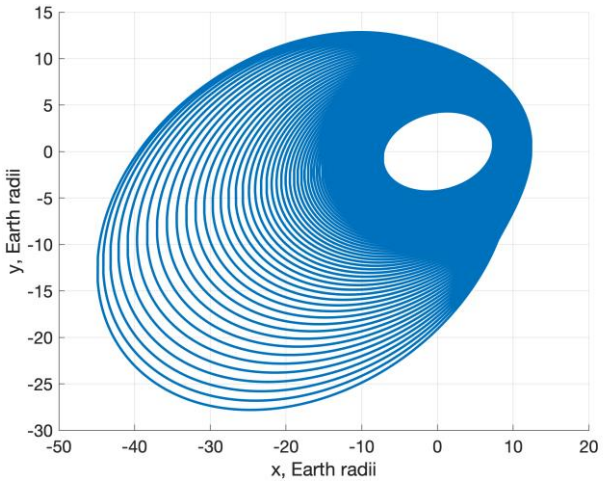

a) xy-projection

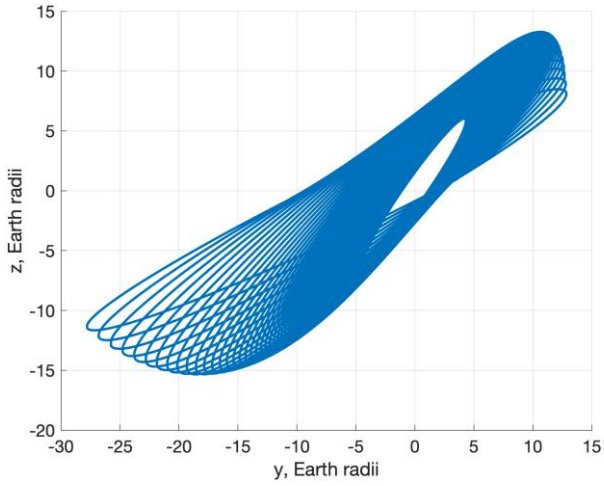

b) yz-projection

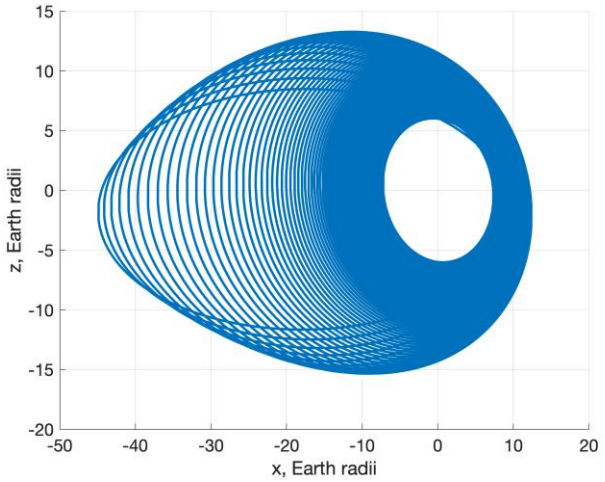

c) xz-projection

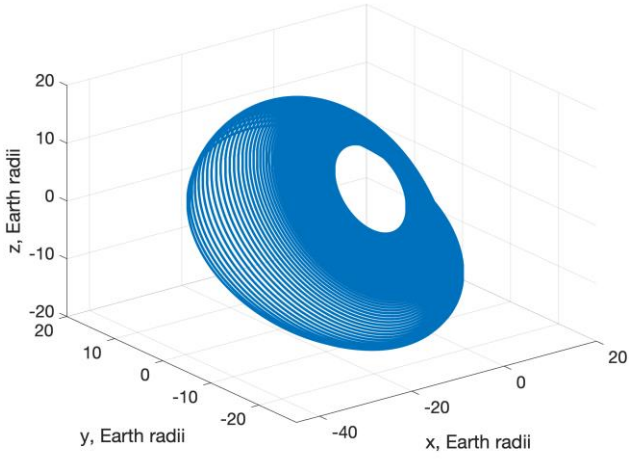

d) 3D view

Fig. 7. The energy-optimal second leg of the transfer trajectory with the launch date of October 1, 2024

What concerns the perturbation effect due to the Sun varying throughout the year, its role appears to be small. It can be explained by the fact that the spacecraft moves in the interior part of the Earth-Moon system; it does not make an excursion far away from the lunar orbit. This is in sharp contrast to weak stability boundary trajectories, also named ballistic lunar transfer trajectories.

4.4 Resonant encounters effect

Up to this moment, all the results are related to time-optimal solutions. To assess the achievable fuel savings, we also designed energy-optimal solutions ended with a series of resonant encounters with the Moon (the 3:1 → 2:1 chain). The second leg of the sample energy-optimal trajectory with the launch date of October 1 is shown in Fig. 7, a-d. Both the 3D view of the spiral trajectory and the projections onto the coordinate planes of the inertial geocentric reference frame (J2000) are displayed. About 41% of the fuel appears to be saved on the second leg of the trajectory compared to the time-optimal solution—in expense of 7 additional months of flight, almost three of which are required for jumping between the resonances. In terms of the pre-launch mass, the fuel savings amount to 3%. A third of savings is due to resonant encounters.

It is worth noting that both the time of flight and the number of revolutions the microspacecraft completes on the second stage of transfer are selected so that the level of maximum thrust acceleration for the obtained energy-optimal solution (Fig. 8) is consistent with the thrust-to-weight ratio available at launch. For the sample transfer shown in Fig. 7, those parameters are respectively set to 290 days and 90 revolutions. The restriction on the level of maximum thrust acceleration is conservative and can be slightly relaxed, which results in a shorter second leg of transfer.

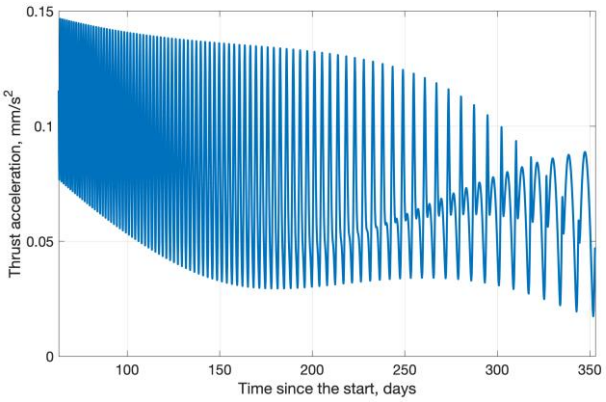

Fig. 8. Energy-optimal control (thrust acceleration) on the 290-day second leg of the transfer trajectory

5. Conclusions

Several most promising scenarios of microspacecraft self-delivery to a near-polar orbit around the Moon have been considered. Based on the standard incoming power level affordable for a microspacecraft of 30-40 kg, three dynamical scenarios were formed differing in the thrust-to-weight ratio and the specific impulse. For the transfer scheme with intermediate capture into a proper lunar L1 halo orbit, low-thrust spiral trajectories starting at one of the popular and easily accessible near-Earth orbits, GTO or MEO, have been numerically optimized over a range of launch dates. While the fuel costs for GTO and MEO are comparable, the latter orbit is better suited for a low-thrust lunar transfer: a less hostile radiation environment allows installing lighter shielding on board.

Transfer performance variations primarily depend on the relative orientation of the initial orbit and lunar orbit planes (determined by the start time) and on the position of the Moon on its orbit (determined by the launch date). For the critical second leg of time-optimal trajectories, a variation in the fuel consumption with changing the start time amounts to 40%, while variations induced by lunar gravity are up to 10%.

Energy-optimal solutions, especially if incorporating lunar resonant encounters, are able to reduce the transfer cost by 30-40% (on the second leg of transfer trajectory), though in expense of twice as long flight time as a time-optimal solution provides.

The final phase of the transfer scheme adopted in the study (the halo orbit-lunar orbit transfer) is independent of the previous phases and can be analyzed separately. It takes approximately 4 months to enter a near-polar lunar orbit with a perilune of 1000 km. Almost 3% of the pre-departure spacecraft mass should be reserved for that.

Acknowledgements

The study is fully supported by the Russian Science Foundation (RSF) grant 19-11-00256.

References

[1] A. Heaton, R. Sood, Space Launch System Departure Trajectory Analysis for Cislunar and Deep Space Exploration, AAS 20-604, AAS/AIAA Astrodynamics Specialist Conference (virtual), 2020, 9–12 August.

[2] G. Racca, A. Marini, L. Stagnaro et al., SMART-1 Mission Description and Development Status, Planetary and Space Science 50 (2002) 1323–1337.

[3] J. Schoenmakers, Post-Launch Optimisation of the SMART-1 Low-Thrust Trajectory to the Moon, ESA SP-548, 18th International Symposium on Space Flight Dynamics, Munich, Germany, 2004, 11–15 October.

[4] M. Shirobokov, S. Trofimov, Low-Thrust Transfers to Lunar Orbits from Halo Orbits Around Lunar Libration Points L1 and L2, Cosmic Research 58 (2020) 181–191.

[5] M. Shirobokov, S. Trofimov, Parametric Analysis of Low-Thrust Lunar Transfers with Resonant

Encounters, Advances in the Astronautical Sciences 158 (2016) 579–603.
[6] M. Shirobokov, S. Trofimov, M. Ovchinnikov, Pareto-Optimal Low-Thrust Lunar Transfers with Resonant Encounters, Advances in the Astronautical Sciences 161 (2018) 485–498.
[7] SPENVIS: SPace ENVironment Information System, https://www.spenvis.oma.be/ (accessed 28.09.20).